

Low bandgap EDOT-quinoxaline and EDOT-thiadiazol-quinoxaline conjugated polymers: Synthesis, redox, and photovoltaic device

Guobing Zhang^a, Yingying Fu^b, Qing Zhang^{a,*}, Zhiyuan Xie^{b,*}

^a Department of Polymer Science and Engineering, School of Chemistry and Chemical Engineering, Shanghai Jiao Tong University, Shanghai, China

^b State Key Laboratory of Polymer Physics and Chemistry, Changchun Institute of Applied Chemistry, Chinese Academy of Science, Changchun, China

ARTICLE INFO

Article history:

Received 25 December 2009

Received in revised form

15 March 2010

Accepted 27 March 2010

Available online 8 April 2010

Keywords:

Polymer solar cells

Ethylendioxythiophene

Low bandgap polymer

ABSTRACT

Three new low bandgap conjugated copolymers with 3,4-ethylenedioxythiophene (EDOT) as donor and 2,3-bis(4-octyloxyphenyl)-quinoxaline (**P1**), 2,3-bis(4-octyloxyphenyl)-thiadiazol-quinoxaline (**P2**, **P3**) as acceptors were synthesized by Stille cross-coupling reaction, and their optical and electrochemical properties were studied. These polymers exhibited optical bandgap of 1.77, 1.29 and 1.13 eV, for **P1**, **P2** and **P3**, respectively. Photovoltaic cells with device configuration of ITO/PEDOT: PSS/Copolymer: PCBM (1:4 w/w)/LiF/Al were fabricated. The measurements revealed an open-circuit voltage (V_{oc}) of 0.52 V, short-circuit current density (J_{sc}) of 3.24 mA/cm² and power conversion efficiency (PCE) of 0.60% for **P1**, and showed a V_{oc} of 0.33 V, J_{sc} of 2.11 mA/cm², PCE of 0.39% for **P2**.

© 2010 Elsevier Ltd. All rights reserved.

1. Introduction

Conjugated copolymers with alternating donor–acceptor repeating units have been widely studied as low bandgap organic semiconductor materials [1–4]. Polymers with various combinations of donors and acceptors have been synthesized for optoelectronic applications, including organic field-effect transistors, organic photovoltaics, and organic light emitting diodes [5–10]. 3,4-Ethylenedioxythiophene (EDOT) has been chosen as an effective donor unit due to its strong electron donating effects and small steric interaction between repeating units in polymers [11–14]. Many electron acceptor units have been polymerized with EDOT to form low bandgap copolymers [7,15–18]. Recently, quinoxaline and thiadiazol-quinoxaline received much attention as acceptor units for synthesis of low bandgap polymers [19,20]. The absorption spectra of polymers with fluorene, thiophene unit as the donor and with thiadiazol-quinoxaline unit as the acceptor were extended to the near-infrared region [21,22]. Conjugated polymers that absorb both in the visible and in the near-infrared regions are considered as good candidates for polymer solar cell applications [23–25].

EDOT/benzothiadiazole copolymer and EDOT/quinoxaline oligomer have been synthesized in the past [6,7]. However, the donor–acceptor type copolymers of EDOT/quinoxaline and

EDOT/thiadiazol-quinoxaline have never been reported. In this paper, we reported the first synthesis, photophysical, and electrochemical properties of three conjugated polymers containing EDOT as donor and quinoxaline, thiadiazol-quinoxaline as acceptors. They are poly[(EDOT)-alt-2,3-bis(4-octyloxyphenyl)-quinoxaline] (**P1**), poly[(EDOT)-alt-2,3-bis(4-octyloxyphenyl)-thiadiazol-quinoxaline] (**P2**), and random poly[(EDOT)-2,3-bis(4-octyloxyphenyl)-thiadiazol-quinoxaline] (**P3**) with increased EDOT content. These donor–acceptor copolymers exhibit broad absorption bands in the visible and near-infrared region and have low bandgaps (1.77 eV for **P1**, 1.29 eV for **P2**, and 1.13 eV for **P3**). Bulk heterojunction solar cells devices based on these polymers as hole transport materials were studied. The power conversion efficiencies of the polymer solar cells are 0.60% for **P1**, 0.39% for **P2**, and 0.11% for **P3** under the illumination of AM 1.5 G, 100 mW/cm².

2. Experimental section

2.1. Materials

n-Butyllithium, tributyltin chloride, sodium borohydride and triphenylarsine were obtained from Alfa Aesar Chemical Company. Tris(dibenzylideneacetone)dipalladium, EDOT, and 4,4'-dimethoxybenzyl were purchased from Sigma–Aldrich Chemical Company. All materials were used as received without further purification. Tetrahydrofuran (THF) and diethyl ether were freshly distilled over

* Corresponding authors.

E-mail addresses: qz14@sjtu.edu.cn (Q. Zhang), xiezy_n@ciac.jl.cn (Z. Xie).

Na wire under nitrogen prior to use. 2,5-Bis(tributylstannyl)-EDOT (**1**) [26], 4,7-dibromobenzothiadiazol (**2**) [27], 3,6-dibromo-1,2-phenylenediamine (**3**) [6], 4,7-dibromo-5,6-dinitro-benzothiadiazole (**4**) [20,27], benzol[1,2,5]thiadiazole-5,6-diamine (**5**) [28], 4,4'-dihydroxybenzil (**6**), 4,4'-bis(octyloxy)benzil (**7**) [29], and 2,5-dibromo-3,4-ethylenedioxythiophene (DBEDOT) [30] were synthesized according to the literature procedures. All the reactions were carried out under nitrogen atmosphere.

2.2. Characterization

Nuclear Magnetic Resonance spectra were recorded either on a Mercury plus 400 MHz machine or on a 300 MHz machine. Gel permeation chromatography (GPC) analyses were performed on a Perkin Elmer Series 200 gel coupled with refractive index detector using THF as eluent with polystyrene as standards. Thermogravimetric analysis (TGA) was conducted with a TA instrument Q5000IR at a heating rate of 20 °C min⁻¹ under nitrogen gas flow. Differential scanning calorimetry (DSC) analysis was performed on a TA instrument Q2000 in a nitrogen atmosphere. All the samples (about 10.0 mg in weight) were first heated up to 250 °C and held for 2 min to remove thermal history, followed by the cooling rate of 20 °C/min to 20 °C and then heating rate of 20 °C/min to 250 °C in all cases. UV–vis absorption spectra were recorded on a Perkin Elmer model λ 20 UV–vis spectrophotometer. Electrochemical measurements were conducted under nitrogen in a deoxygenated anhydrous acetonitrile solution of *tetra-n*-butylammonium hexafluorophosphate (0.1 M), using a BAS 100B electrochemical analyzer. A platinum electrode was used as a working electrode, a platinum-wire was used as an auxiliary electrode, and a silver wire anodized with AgCl was used as a reference electrode, thin

polymer film was coated on platinum electrode. Ferrocene was added as an internal reference.

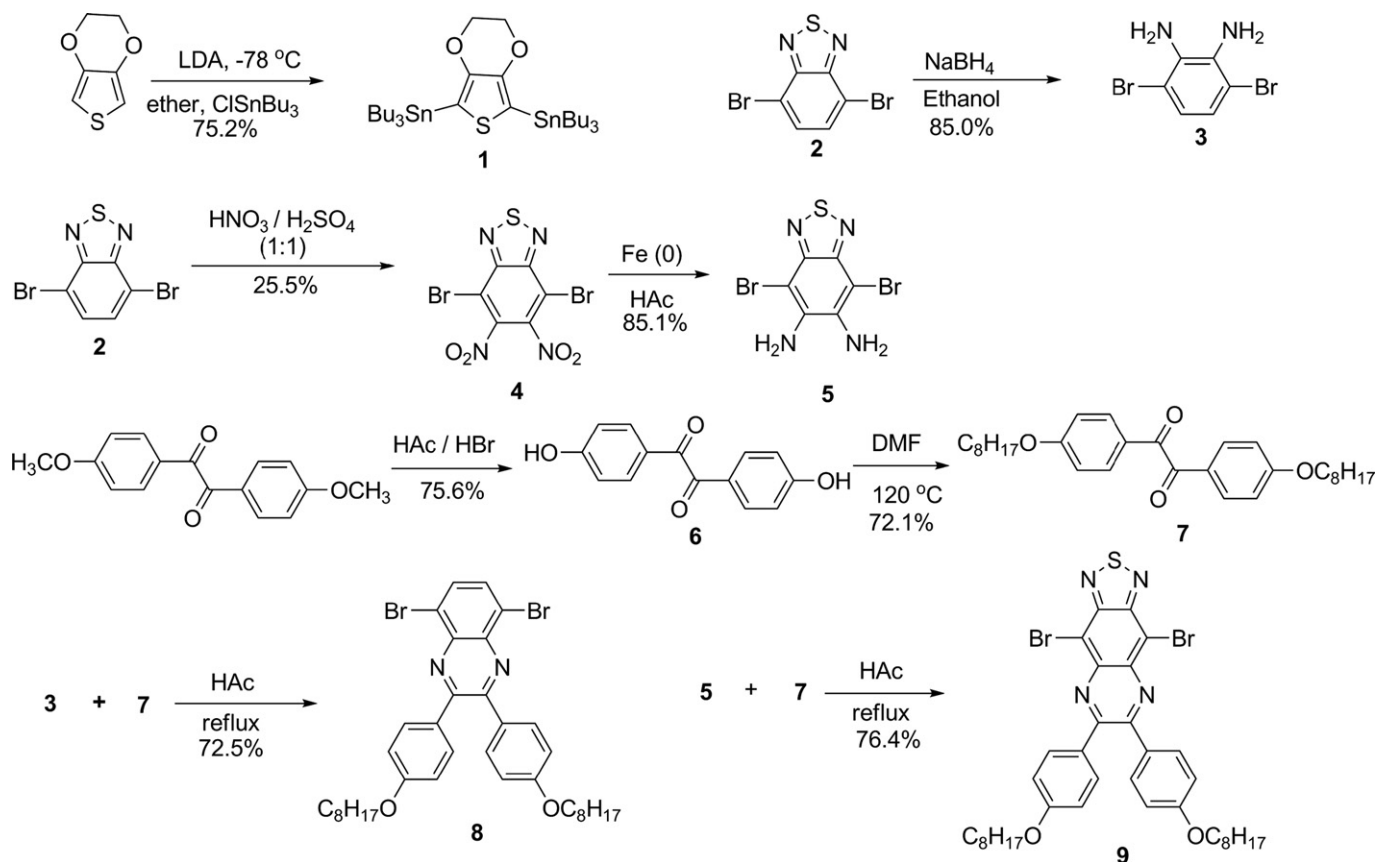
2.3. Device fabrication

Polymer solar cells (PSCs) with the device structures of ITO/PEDOT: PSS/polymer: PCBM (1:4, w/w)/LiF/Al were fabricated as follows: a ca. 40-nm-thick PEDOT: PSS (Baytron P AI 4083) was spin-coated from an aqueous solution onto the pre-cleaned ITO substrates, followed by drying at 120 °C for 30 min in air. Then the substrates were transferred into a nitrogen filled glove box. The prepared solution containing a mixture of polymer: PCBM (5 mg/mL:20 mg/mL) in chlorobenzene was spin-coated on top of the PEDOT/PSS layer. Finally the samples were transferred into an evaporator and 1-nm-thick LiF and 100-nm-thick Al were thermally deposited under a vacuum of 10⁻⁶ Torr with area of 0.12 cm². The devices were encapsulated in the glove box and measured in the air. Current–voltage characteristics were measured using a computer controlled Keithley 236 source meter. The photocurrent was measured under AM 1.5 G illumination at 100 mW/cm² from a solar simulator (Oriel, 91160A-1000).

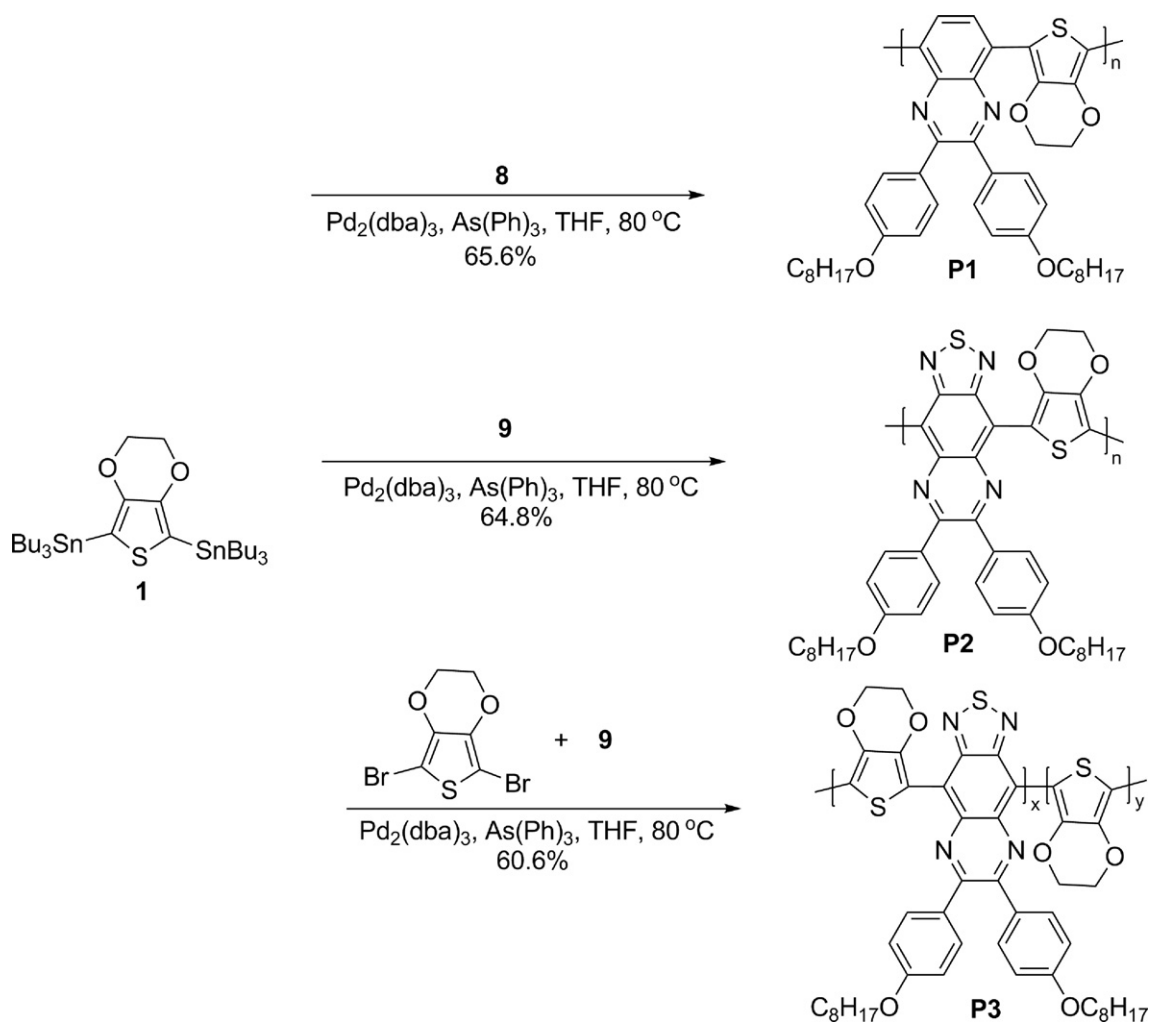
2.4. Synthesis of polymer

2.4.1. 2,3-Bis(4-octyloxyphenyl)-5,8-dibromoquinoxaline (**8**)

A solution of 3,6-dibromo-1,2-phenylenediamine (**3**) (1.0 g, 3.76 mmol) and 4,4'-bis(octyloxy)benzil (**7**) (1.75 g, 3.76 mmol) in acetic acid (100 mL) was refluxed overnight. After the mixture was cooled to 0 °C, ethanol (200 mL) was added to the solution. The precipitate was isolated by filtration and was washed with ethanol to afford the desired compound (1.89 g, 72.5%). ¹H NMR (400 MHz,



Scheme 1. Synthetic routes of monomers 1–9.

Scheme 2. Synthetic routes of **P1**, **P2**, and **P3**.

CDCl_3): $\delta = 7.85$ (s, 2H), 7.65 (d, $J = 8.0$ Hz, 4H), 6.88 (d, $J = 8.8$ Hz, 4H), 3.99 (t, $J = 6.4$ Hz, 4H), 1.80 (m, 4H), 1.46 (m, 4H), 1.30 (m, 16H), 0.90 (t, $J = 6.4$ Hz, 6H). ^{13}C NMR (100 MHz, CDCl_3): $\delta = 160.69$, 153.80, 139.24, 132.70, 131.88, 130.54, 123.66, 114.59, 68.33, 32.04, 29.58, 29.46, 29.43, 26.25, 22.88, 14.33. Anal. Calcd for $\text{C}_{36}\text{H}_{44}\text{Br}_2\text{N}_2\text{O}_2$ (%): C, 62.07; H, 6.37; N, 4.02. Found (%): C, 62.33; H, 6.39; N, 3.54.

2.4.2. 2,3-Bis(4-octyloxyphenyl)-5,8-dibromothiadiazol-quinoxaline (**9**)

A solution of benzol[1,2,5]thiadiazole-5,6-diamine (**5**) (1.00 g, 3.09 mmol) and 4,4'-bis(octyloxy)benzil (**7**) (1.44 g, 3.09 mmol) in acetic acid (100 mL) was refluxed overnight. The mixture was cooled to room temperature. Ethanol (200 mL) was added to the solution and the precipitate was filtrated and washed with ethanol several times to afford a red solid (1.78 g, 76.4%). ^1H NMR (400 MHz, CDCl_3): $\delta = 7.75$ (d, $J = 8.8$ Hz, 4H), 6.91 (d, $J = 8.8$ Hz, 4H), 4.01 (t, $J = 6.8$ Hz, 4H), 1.80 (m, 4H), 1.44 (m, 4H), 1.30 (m, 16H), 0.90 (t, $J = 6.4$ Hz, 6H). ^{13}C NMR (100 MHz, CDCl_3): $\delta = 161.50$, 155.69, 152.35, 138.26, 132.19, 130.19, 114.62, 113.48, 68.43, 32.04, 29.58, 29.47, 29.40, 26.25, 22.89, 14.34. Anal. Calcd for $\text{C}_{36}\text{H}_{42}\text{Br}_2\text{N}_4\text{O}_2\text{S}$ (%): C, 57.30; H, 5.61; N, 7.42. Found (%): C, 57.18; H, 5.54; N, 7.14.

2.4.3. Synthesis of **P1** by Stille coupling reaction

Tris(dibenzylideneacetone)dipalladium (0.017 g, 0.018 mmol), triphenylarsine (0.011 g, 0.036 mmol) were added to a solution of

2,5-bis(tributylstannyl)-EDOT (**1**) (0.66 g, 0.92 mmol) and 2,3-bis(4-octyloxyphenyl)-5,8-dibromothiadiazol-quinoxaline (**8**) (0.64, 0.92 mmol) in THF (15 mL) under nitrogen. The solution was subjected to three cycles of evacuation and nitrogen refilling. After degassing, the reaction vessel was sealed. The reaction was heated to 80 °C for 72 h. After cooling to room temperature, aqueous potassium fluoride solution (20 mL, 1.0 M) was added and the mixture was stirred for 1 h. The mixture was extracted with dichloromethane (3 \times). The combined organic layer was dried over anhydrous sodium sulfate and filtered. The filtrate was concentrated at about 10 mL in vacuum. The solution was added slowly to methanol (250 mL) with stir. The purple precipitate was collected by filtration. The product was further purified by washing with methanol, hexane and then extracted with chloroform using a Soxhlet extractor. After removing solvent and drying in vacuum overnight at 45 °C, the polymer was obtained as a purple powder (0.41 g, 65.6%). ^1H NMR (400 MHz, CDCl_3): $\delta = 8.55$ –8.62 (br, 2H), 7.62–7.72 (br, 4H), 6.52–6.64 (br, 4H), 4.45–4.60 (br, 4H), 3.72–3.82 (br, 4H), 1.58–1.70 (br, 4H), 1.15–1.40 (br, 20 H), 0.78–0.92 (br, 6H). ^{13}C NMR (75 MHz, CDCl_3): $\delta = 159.83$, 150.54, 140.17, 137.73, 132.05, 131.43, 129.50, 128.78, 116.70, 114.22, 68.15, 64.90, 32.02, 29.63, 29.44, 26.33, 26.22, 22.86, 14.32. $M_n = 16.8$ kDa, PDI = 1.14.

2.4.4. Synthesis of **P2** by Stille coupling reaction

Same polymerization method was used as **P1**. Compound used were 2,3-bis(4-octyloxyphenyl)-5,8-dibromothiadiazol-quinoxaline

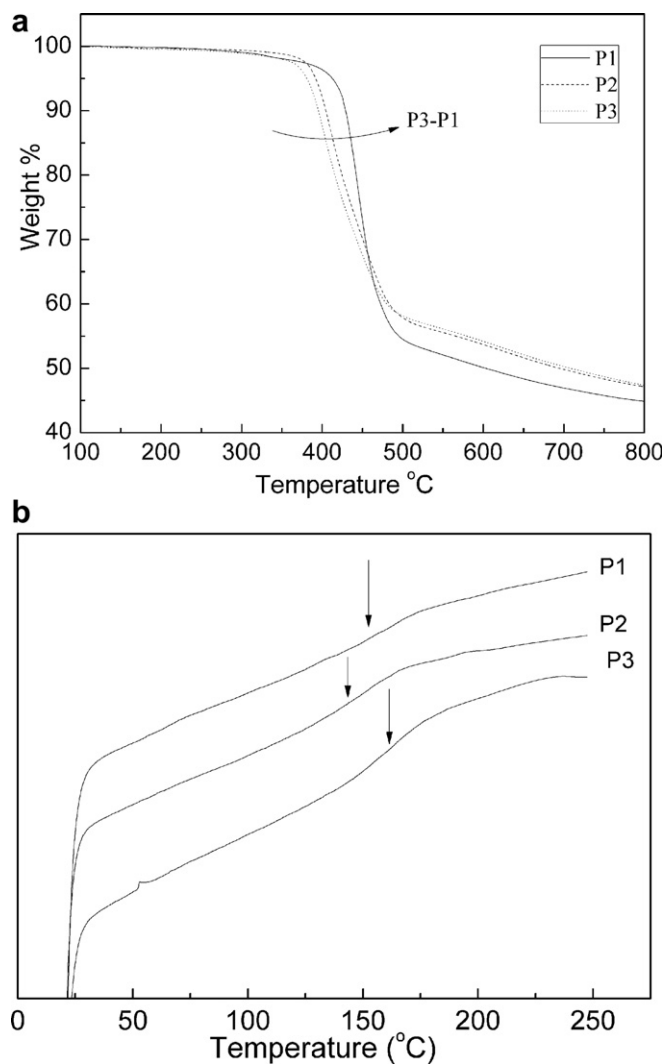


Fig. 1. (a) TGA curves and (b) DSC curves of three copolymers **P1**, **P2**, and **P3**.

(**9**) (0.89 g, 1.18 mmol), 2,5-bis(tributylstannyl)-EDOT (**1**) (0.85 g, 1.18 mmol) THF (15 mL), tris(dibenzylideneacetone)dipalladium (0.022 g, 0.024 mmol), and triphenylarsine (0.014 g, 0.048 mmol) in this polymerization reaction. After same workup as **P1**, a black-green powder was obtained (0.56 g, yield, 64.8%). $^1\text{H NMR}$ (400 MHz, CDCl_3): $\delta = 7.85\text{--}7.98$ (br, 4H), 6.84–6.96 (br, 4H), 4.48–4.58 (br, 4H), 3.94–4.06 (br, 4H), 1.74–1.86 (br, 4H), 1.40–1.52 (br, 4H), 1.23–1.38 (br, 16H), 0.84–0.93 (br, 6H). $^{13}\text{C NMR}$ (75 MHz, CDCl_3): $\delta = 160.53$, 152.94, 152.47, 141.24, 136.74, 132.01, 131.20, 120.56, 115.44, 114.18, 68.33, 64.89, 31.01, 29.36, 29.23, 26.05, 22.66, 14.35. (**Note**: two peaks in $^{13}\text{C NMR}$ spectrum overlap). Mn = 22.4 kDa, PDI = 1.16.

Table 1
Optical and redox properties of **P1**, **P2**, and **P3**.

Polymer	Solution		Film		Film		
	$\lambda_{\text{max}}^{\text{abs}}$ (nm)	$\lambda_{\text{max}}^{\text{abs}}$ (nm)	$\lambda_{\text{onset}}^{\text{abs}}$ (nm)	E_g^{opta} (eV)	$E_{\text{onset}}^{\text{red}}$ (V)	EA ^b (eV)	IP ^c (eV)
P1	584	598	700	1.77	−1.15	−2.99	−4.76
P2	738	760	960	1.29	−0.55	−3.59	−4.88
P3	769	796	1100	1.13	−0.53	−3.61	−4.74

^a E_g^{opt} was estimated from UV–vis absorption onset.

^b EA was obtained based on EA = $-(E_{\text{onset}}^{\text{red}} + 4.14)$ eV.

^c IP was obtained based on IP = EA − E_g^{opt} eV.

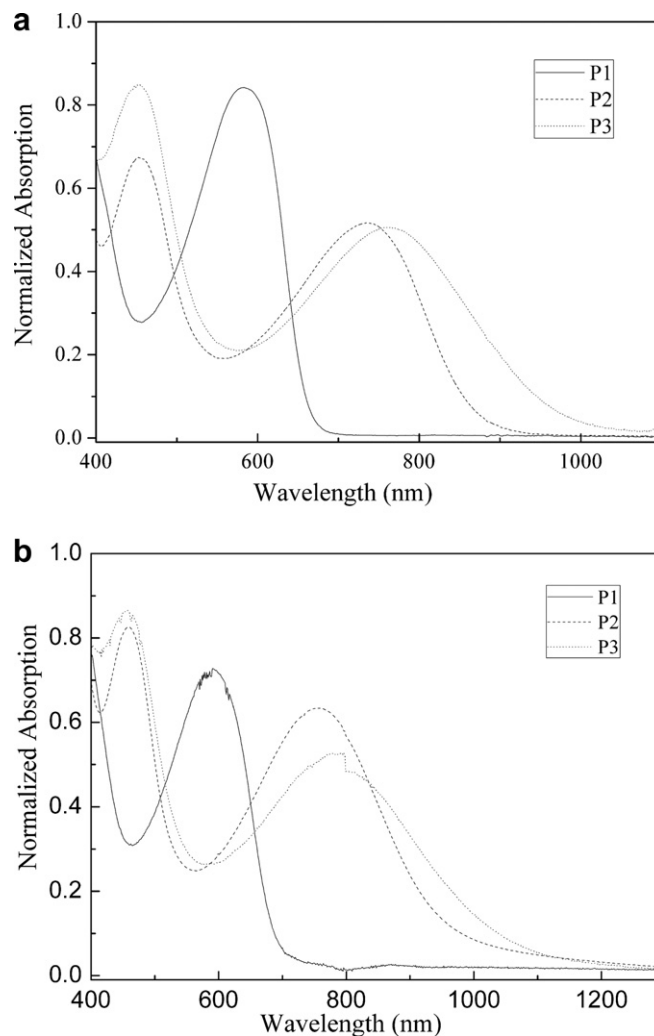


Fig. 2. Normalized UV–vis spectra of **P1**, **P2** and **P3** (a) in chloroform solution and (b) as thin film.

2.4.5. Synthesis of **P3** by Stille coupling reaction

Same polymerization method was used as **P1**. 2,3-Bis(4-octyloxyphenyl)-5,8-dibromothiadiazo-quinoxaline (**9**) (0.57 g, 0.75 mmol), 2,5-bis(tributylstannyl)-EDOT (**1**) (0.90 g, 1.25 mmol), 2,5-dibromo-EDOT (DBEDOT) (0.15 g, 0.50 mmol), THF (20 ml), tris(dibenzylideneacetone)dipalladium (0.023 g, 0.025 mmol), and triphenylarsine (0.015 g, 0.05 mmol) were used in this polymerization. After same workup as **P1**, a black powder was obtained (0.75 g, yield, 60.6%). $^1\text{H NMR}$ (400 MHz, CDCl_3): $\delta = 7.72\text{--}7.98$ (br, 4H), 6.80–6.96 (br, 4H), 4.20–4.68 (br, 8H), 3.94–4.04 (br, 4H), 1.73–1.87 (br, 4H), 1.42–1.52 (br, 4H), 1.22–1.40 (br, 16H), 1.83–0.94 (br, 6H). $^{13}\text{C NMR}$ (75 MHz, CDCl_3): $\delta = 160.77$, 152.95, 152.87, 141.48, 136.98, 132.24, 132.04, 131.62, 131.44, 121.35, 115.69, 114.41, 68.35, 65.35, 64.99, 32.06, 29.95, 29.62, 29.49, 26.30, 22.91, 14.37. Mn = 23.2 kDa, PDI = 1.62.

3. Results and discussion

3.1. Synthesis of the polymers

The synthetic routes for monomers are depicted in Scheme 1. The 2,5-bis(tributylstannyl)-EDOT (**1**) was prepared from EDOT according to our previous work [26]. The 4,7-dibromobenzothiadiazol (**2**) was obtained from 2,1,3-benzothiadiazole in the presence of HBr/Br₂ mixture according to reported method [27] and

compound **2** was reduced with an excess amount of sodium borohydride to give 3,6-dibromo-1,2-phenylenediamine (**3**) as a pale yellow solid [6]. Nitration of **2** in 1/1 (vol/vol) of fuming nitric acid and fuming sulfuric acid gave 4,7-dibromo-5,6-dinitro-benzothiadiazole (**4**) in 25.5% yield after recrystallization in ethanol. Reduction of **4** with iron dust in acetic acid resulted in diamine **5**. 4,4'-dihydroxybenzil (**6**) was prepared from 4,4'-dimethoxybenzil in the HBr/HAC mixture as a light tan solid. Compound **6** was reacted with 1-bromooctane in DMF to afford diketone **7** in 72.1% yield. The condensation of diketone **7** with diamine **3** and **5** in acetic acid gave the monomer **8** and **9**.

The polymerization of **P1**, **P2**, and **P3** were depicted in Scheme 2. Alternating copolymer **P1** and **P2** were prepared by Stille coupling reaction with 1:1 monomer ratio in the presence of $\text{Pd}_2(\text{dba})_3$ as catalyst and triphenylarsine as ligand to give **P1** (yield 65.6%) and **P2** (yield 64.8%). The crude copolymers were purified by precipitating in methanol and then by washing with hexane and methanol in a Soxhlet extractor. Random copolymer **P3** was prepared by using the same polymerization method as copolymer **P1** and **P2** but with 2,5-bis(tributylstannyl)-EDOT (**1**), 2,3-bis(4-octyloxyphenyl)-5,8-dibromothiadiazol-quinoxaline (**9**), and DBEDOT. Those copolymers are soluble in common organic solvents such as chloroform, dichloromethane, and THF at room temperature. The number average molecular weights (M_n) of the copolymers were 16.8–23.2 kDa with a polydispersity of 1.14–1.62.

3.2. Thermal stability

Thermal stability of copolymers was investigated by thermogravimetric analysis (TGA). The TGA plots of **P1**, **P2**, and **P3** were showed on Fig. 1a. The thermal decomposition temperatures for **P1**, **P2** and **P3** were determined as 410 °C, 392 °C, and 380 °C, respectively choosing 5 wt% weight loss as the onset loss point. Three copolymers displayed adequate thermal stability for application in polymer solar cells and other optoelectronic devices. The DSC curves of copolymers are shown in Fig. 1b. All three copolymers had glass transition points. The glass transition temperatures of **P1**, **P2**, and **P3** are 152 °C, 143 °C, and 162 °C, respectively.

3.3. Optical properties

The optical absorption properties of the three copolymers were listed in Table 1. UV–vis spectra were measured both in chloroform solutions (Fig. 2a) and as thin films on glass slides (Fig. 2b). As shown in Fig. 2a, the UV–vis spectrum of **P1** shows an absorption peak ($\lambda_{\text{max}}^{\text{abs}}$) at 584 nm. **P2** shows an absorption peak ($\lambda_{\text{max}}^{\text{abs}}$) at 738 nm, and **P3** shows an absorption peak ($\lambda_{\text{max}}^{\text{abs}}$) at 769 nm. **P2** and **P3** had 154 nm and 185 nm red-shifted respectively compared to that of **P1**. Such red-shift in absorption can be explained by the fact that the thiadiazol-quinoxaline units are stronger acceptors than the quinoxaline unit. The UV–vis spectra of **P1**, **P2** and **P3** as thin film were showed in Fig. 2b. The thin film absorption spectra of all three copolymers have much more broad absorption range than solution absorption spectra. The UV–vis spectra of **P1**, **P2** and **P3** as thin film show a $\lambda_{\text{max}}^{\text{abs}}$ at 598 nm, 760 nm and 796 nm, and the $\lambda_{\text{max}}^{\text{abs}}$ of **P1**, **P2**, and **P3** have red-shifted 14–27 nm relative to copolymers in solutions. The significant red-shift suggests the copolymers aggregate very well in solid state. The optical bandgap was calculated to be 1.77 eV (absorption edge: ~700 nm) for **P1** and 1.29 eV for **P2** (absorption edge: ~960 nm), while the absorption of **P3** was more broad and the absorption edge extended to 1100 nm, the optical bandgap of **P3** was calculated to be 1.13 eV.

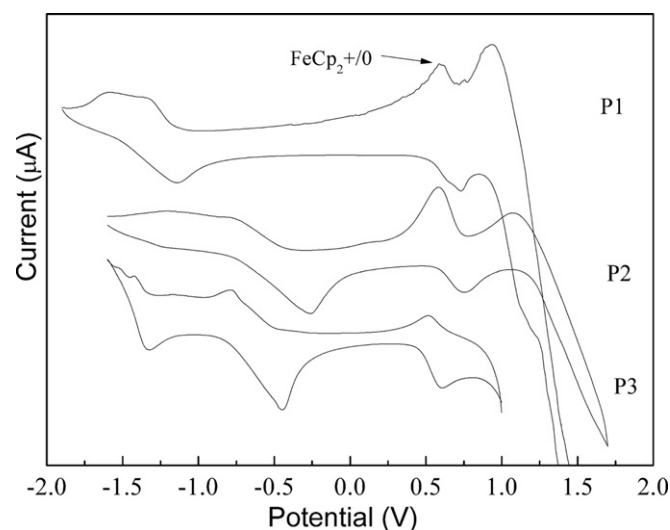


Fig. 3. Cyclic voltammograms of copolymers thin film (**P1**, **P2** and **P3**) on a platinum electrode in 0.1 M $\text{Bu}_4\text{NPF}_6/\text{MeCN}$ at a scan rate of 50 mV s^{-1} with FeCp_2 as internal standard.

3.4. Electrochemical studies

The electrochemical redox behavior of the conjugated polymers was investigated by cyclic voltammetry (CV). The cyclic voltammograms of **P1**, **P2** and **P3** were shown in Fig. 3. All the redox data were summarized in Table 1. The potentials were internally referenced to the ferrocene/ferrocenium redox couple (Fc/Fc^+), which assumed the redox potential of ferrocene/ferrocenium has an absolute energy level of 4.8 eV to vacuum [31–33]. The potential of Fc/Fc^+ was measured as 0.66 V. The lowest unoccupied molecular orbital (LUMO) energy levels of polymers were calculated from the $E_{\text{onset}}^{\text{red}}$ and highest occupied molecular orbital (HOMO) energy levels were obtained based formula: $\text{HOMO} = \text{LUMO} - E_g^{\text{opt}}$. Both **P1** and **P2** exhibit one reversible n-doping/dedoping (reduction/reoxidation) processes in the negative potential region, while **P3** has two reversible n-doping/dedoping processes, however, no distinct oxidation wave was observed in the positive potential range. The $E_{\text{onset}}^{\text{red}}$ is -1.15 V for **P1**, -0.55 V for **P2**, and -0.53 V for **P3**, from which we can estimate the EA values (LUMO energy levels) of -2.99 , -3.59 , and -3.61 eV for **P1**, **P2**, and **P3**, respectively. From the E_g^{opt} and LUMO, the IP values (HOMO energy levels) of -4.76 eV for **P1**, -4.88 eV for **P2**, and -4.74 eV for **P3** were estimated. In order to make a clear comparison, the results of HOMO and LUMO

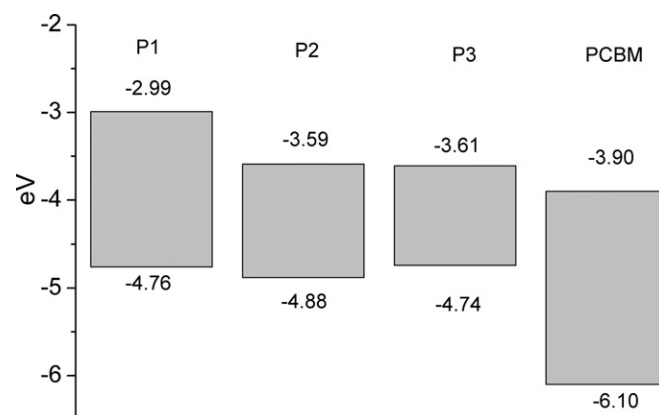


Fig. 4. Energy level diagrams for **P1**, **P2** and **P3**.

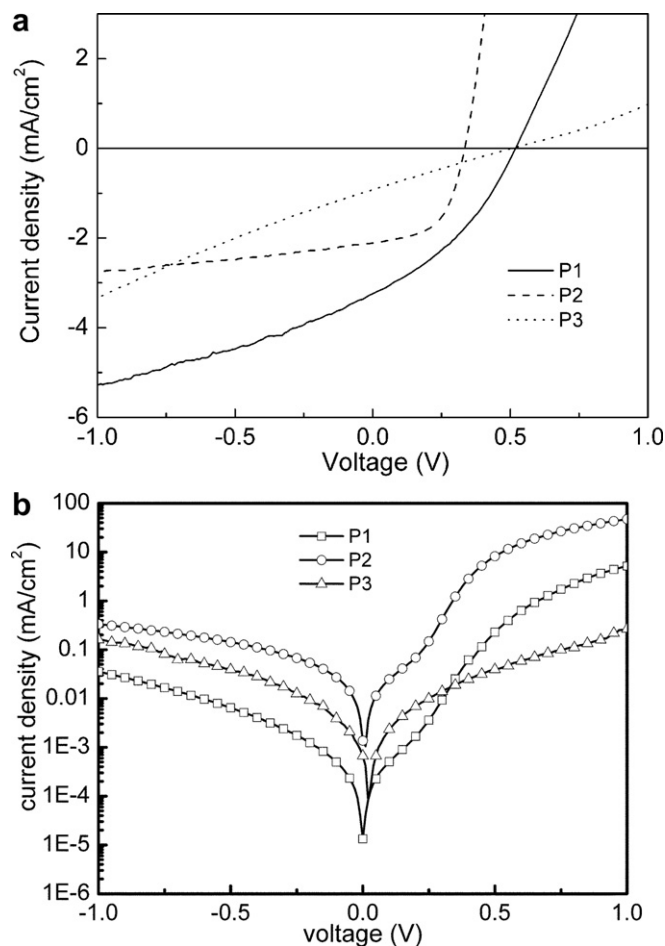


Fig. 5. Current–voltage characteristics of polymers/PC₆₀BM solar cells (a) under illumination (AM 1.5 G, 100 mW/cm²) and (b) dark condition.

energy levels of **P1**, **P2** and **P3** were summarized in Fig. 4. The HOMO energy levels of the three polymers are very close. The HOMO energy levels are relatively too high for polymers as donor materials in bulk heterojunction solar cell devices with PCBM as acceptor. The LUMO energy level of **P1** is about 0.91 eV higher and **P2**, **P3** are 0.31 and 0.29 eV higher than that of PCBM (−3.90 eV) [34]. **P2** and **P3** have relatively low LUMO energy level compared to **P1** because the strong electron-withdrawing units in **P2** and **P3** reduced the LUMO energy level of polymers [35].

3.5. Characterization of polymer solar cells

The polymer solar cells (PSCs) were fabricated with the device structures of ITO/PEDOT: PSS/polymer: PCBM/LiF/Al. The active layer of polymer and PCBM blend was prepared by spin-coating the chlorobenzene solution of the polymers and PCBM (1:4, w/w) on the ITO/PEDOT: PSS electrode. The current density–voltage characteristics with and without illumination were shown in Fig. 5.

Table 2
Characteristic properties of polymers solar cells.

Polymers	V_{oc} (V)	J_{sc} (mA/cm ²)	FF (%)	PCE (%)
P1	0.52	3.24	36	0.60
P2	0.33	2.11	55	0.39
P3	0.51	0.92	24	0.11

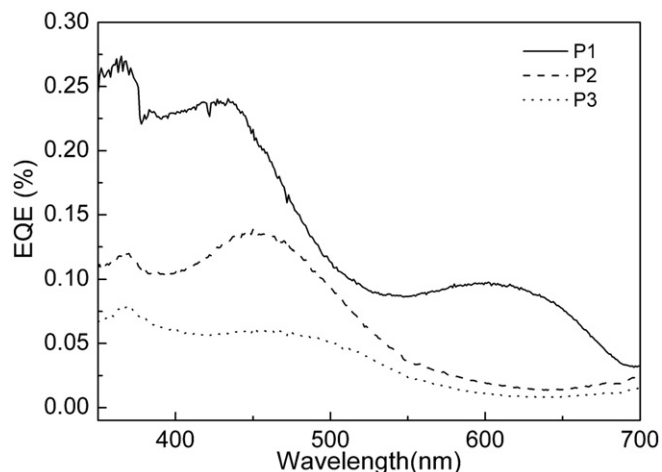


Fig. 6. The external quantum efficiency of polymers/PC₆₀BM.

Representative parameters of solar cells are summarized in Table 2. The device with **P1**: PCBM layers (60 nm) showed an open-circuit voltage (V_{oc}) of 0.52 V, a short-circuit current density (J_{sc}) of 3.24 mA/cm², and a fill factor (FF) of 36%, giving a power conversion efficiency (PCE) of 0.60%. The device with **P2**: PCBM layers (90 nm) demonstrated a V_{oc} value of 0.33 V, a FF of 55%, and a J_{sc} value of 2.11 mA/cm², leading to the PCE value of 0.39%, a slightly decreased performance compare to **P1**. For the BHJ devices made from **P3**: PCBM film (70 nm), the device exhibited almost same V_{oc} value of 0.51 V, and a decreased J_{sc} value of 0.92 mA/cm² compare to the value of **P1** and a FF of 24%, resulting in the significantly decreased PCE of 0.11%. Compare to **P1**, the device with **P2**: PCBM demonstrated a quite lower V_{oc} value of 0.33 V. In our experimental condition, the V_{oc} of solar cells is not only determined by the energy difference between HOMO of the donor and LUMO of the acceptor, but also shows a strong inverse correlation with the dark current [36]. We find that **P2** has much higher dark current than **P1** from Fig. 5b. This may be the reason that the V_{oc} value of **P2** is lower than that of **P1**. The external quantum efficiencies (EQE) of the solar cells based on **P2** and **P3** with PCBM as acceptor were very low, especially above 600 nm (Fig. 6), which resulted in very weak photocurrent. The similar results have been reported by Janssen on related polymer structures [21]. They reported that the EQE of the cell based on thiadiazol-quinoxaline and thiophene copolymer with PCBM acceptor was almost zero above 700 nm. The solar cell based on **P1** and PCBM has relatively high EQE compared to **P2** and **P3**. This is the main reason that solar cell based on **P1** has higher J_{sc} and PCE than those of **P2** and **P3**.

4. Conclusions

New classes of donor/acceptor conjugated polymers comprising EDOT units, quinoxaline units and thiadiazol-quinoxaline units have been successfully synthesized by Stille cross-coupling polymerization method. The copolymers of EDOT and 2,3-bis(4-octyloxyphenyl)-quinoxaline (**P1**), 2,3-bis(4-octyloxyphenyl)-thiadiazol-quinoxaline (**P2**, **P3**) have achieved relatively low bandgap (1.77–1.13 eV). However, the HOMO energy levels of all three polymers are relatively too high for BHJ solar cell devices with PCBM as acceptor to achieve high open-circuit voltage and power conversion efficiency. The performance of photovoltaic cells based on blends of copolymers and PCBM as active layers are moderate. The power conversion efficiencies of 0.60% for **P1**, 0.39% for **P2** and 0.11% for **P3** were obtained.

Acknowledgements

This work was supported by National Nature Science Foundation of China (NSFC Grant no. 20674049 and 20834005) and Shanghai municipal government (Grant no. B202 and 10ZZ15).

Appendix. Supporting information

The supplementary data associated with this article can be found in the on-line version at [doi:10.1016/j.polymer.2010.03.050](https://doi.org/10.1016/j.polymer.2010.03.050).

References

- [1] Steckler TT, Abboud KA, Craps M, Rinzler AG, Reynolds JR. *Chem Commun* 2007;46:4904–6.
- [2] Huo LJ, Zhou Y, Li YF. *Macromol Rapid Commun* 2008;29:1444–8.
- [3] Guo XG, Kim FS, Jenekhe SA, Watson MD. *J Am Chem Soc* 2009;131:7206–7.
- [4] Peet J, Senatore ML, Heeger AL, Bazan GC. *Adv Mater* 2009;21:1521–7.
- [5] Liang YY, Feng D, Wu Y, Tsai ST, Li G, Ray C, et al. *J Am Chem Soc* 2009;131:7792–9.
- [6] Gunbas GE, Durmus A, Toppare L. *Adv Mater* 2008;20:691–5.
- [7] Beaujuge PM, Ellinger S, Reynolds JR. *Adv Mater* 2008;20:2772–6.
- [8] He YJ, Wang X, Zhang J, Li YF. *Macromol Rapid Commun* 2009;30:45–51.
- [9] Jenekhe SA, Lu L, Alam MM. *Macromolecules* 2001;34:7315–24.
- [10] Wu PT, Kim FS, Champion RD, Jenekhe SA. *Macromolecules* 2008;41:7021–8.
- [11] Beaujuge PM, Ellinger S, Reynolds JR. *Nat Mater* 2008;7:796–9.
- [12] Meng H, Tucker D, Chaffins S, Chen Y, Helgeson R, Dunn B, et al. *Adv Mater* 2003;15:146–9.
- [13] Bokria JG, Kummar A, Seshadri V, Tran A, Sotzing GA. *Adv Mater* 2008;20:1175–8.
- [14] Thompson BC, Kim YG, Reynolds JR. *Macromolecules* 2005;38:5359–62.
- [15] Berlin A, Zotti G, Zecchin S, Schiavon G, Vercelli B, Zanelli A. *Chem Mater* 2004;16:3667–76.
- [16] Sonmez G, Meng H, Wudl F. *Chem Mater* 2003;15:4923–9.
- [17] Colladet K, Fourier S, Cleij TJ, Lutsen L, Gelan J, Vanderzande D, et al. *Macromolecules* 2007;40:65–72.
- [18] Lee JY, Heo SW, Choi H, Kwon YJ, Haw JR, Moon DK. *Sol Energ Mater Sol Cell* 2009;93:1932–8.
- [19] Gadisa A, Mammo W, Andersson LM, Admassie S, Zhang FL, Andersson MR, et al. *Adv Funct Mater* 2007;17:3836–42.
- [20] Yi H, Johnson RG, Iraqi A, Mohamad D, Royce R, Lidzey DG. *Macromol Rapid Commun* 2008;29:1804–9.
- [21] Zoombelt AP, Fonrodona M, Wienk MM, Sieval AB, Hummelen JC, Janssen RJ. *Org Lett* 2009;4:903–6.
- [22] Zhang F, Mammo W, Andersson LM, Admassie S, Andersson MR, Inganas O. *Adv Mater* 2006;18:2169–73.
- [23] Wang X, Perzon E, Oswald F, Langa F, Admassie S, Andersson MR, et al. *Adv Funct Mater* 2005;15:1665–70.
- [24] Wienk MM, Turbiez MR, Struijk MP, Fonrodona M, Janssen RJ. *Appl Phys Lett* 2006;511:576–9.
- [25] Wang X, Perzon E, Mammo W, Oswald F, Admassie S, Persson NK, et al. *Thin Solid Films* 2006;511:576–80.
- [26] Wei YF, Zhang Q, Jiang Y, Yu JS. *Macromol Chem Phys* 2009;210:769–75.
- [27] Mancilha FS, Neto BD, Lopes AS, Moreira JR, Quina FH, Goncalves RS, et al. *Eur J Org Chem*; 2006:4924–33.
- [28] Perzon E, Wang XJ, Admassie S, Inganas O, Andersson MR. *Polymer* 2006;47:4261–8.
- [29] Moylan CR, Miller RD, Twieg RJ, Betterton KM, Lee VY, Matray TJ, et al. *Chem Mater* 1993;5:1499–508.
- [30] Meng H, Perepichka DF, Bendikov M, Wudl F, Pan GZ, Yu WJ, et al. *J Am Chem Soc* 2003;125:15151–62.
- [31] He YJ, Zhao GJ, Min J, Zhang MJ, Li YF. *Polymer* 2009;50:5055–8.
- [32] Li YF, Cao Y, Gao J, Wang D, Yu G, Heeger AJ. *Syn Met* 1999;99:243–8.
- [33] Zhan XW, Liu YQ, Wu X, Wang S, Zhu DB. *Macromolecules* 2002;35:2529–37.
- [34] He YJ, Chen HY, Hou JH, Li YF. *J Am Chem Soc* 2010;132:1377–82.
- [35] Cheng YJ, Yang SH, Hsu CS. *Chem Rev* 2009;109:5868–923.
- [36] Perez MD, Borek C, Forrest SR, Thompson ME. *J Am Chem Soc* 2009;131:9281–6.